



# Structural evolution of the central part of the Krušné hory (Erzgebirge) Mountains in the Czech Republic—evidence for changing stress regime during Variscan compression

Jiří Konopásek<sup>a,b,\*</sup>, Karel Schulmann<sup>a</sup>, Ondrej Lexa<sup>a</sup>

<sup>a</sup>Charles University, Institute of Petrology and Structural Geology, Faculty of Science, Albertov 6, 128 43, Praha 2, Czech Republic

<sup>b</sup>Geophysical Institute, Czech Academy of Science, Boční II/1401, 141 31, Prague 4, Czech Republic

Received 12 July 2000; revised 17 December 2000; accepted 19 December 2000

## Abstract

In the central part of the Krušné hory (Erzgebirge) Mountains, the parautochthonous metasedimentary basement has been overthrust by a crustal nappe of fine- and coarse-grained orthogneisses. The thrust boundary is defined by the presence of mafic eclogites with preserved subduction-related fabric. Westward thrusting of an allochthonous unit is associated with the development of the main metamorphic foliation and lineation in non-eclogitic lithologies. Buttressing of the allochthonous body from the west is responsible for the development of late, large-scale folds with N–S trending hinges and vertical axial planes. Subsequent N–S compression leads to large-scale folding of both the parautochthonous and allochthonous units. This deformation produces km-scale antiforms with hinges plunging to the west and is associated with the development of the E–W stretching lineation as a result of complete reworking of earlier fabric in the limb zones. N–S shortening is also associated with the development of small-scale folds and brittle-ductile kink bands suggesting a decrease in temperature, and, thus, uplift of the whole studied area during this event. The last stage of deformation is characterised by the development of kink-band folds and a crenulation cleavage. These structures suggest a sub-vertical direction of principal compression, developed exclusively in those parts of the area in which the N–S compression produced steep planar fabric. © 2001 Elsevier Science Ltd. All rights reserved.

## 1. Introduction

In the western part of the Saxothuringian domain of the Bohemian Massif, the identification of the major tectonic units is relatively easy because of considerable metamorphic contrast between high-grade crystalline rocks and adjacent low-grade metasediments. Here, allochthonous high-grade crystalline units represented by the Münchberg, Frankenberg and Wildenfels klippen are thrust over low-grade Carboniferous sediments (Franke et al., 1995). Another important structural pattern is associated with exhumation of the Saxonian granulites. The emplacement of this body into the upper crust is interpreted in terms of the extension associated with the development of a metamorphic core complex (Franke, 1993).

In the eastern part of the Saxothuringian domain (central and eastern Krušné hory Mountains), the identification of the major structural units is more difficult because of the medium- to high-grade metamorphism affecting both the allochthonous and autochthonous units. Moreover, at least

two periods of high-grade metamorphism have affected the pre-Palaeozoic basement in this area, and it is difficult, if not impossible, to separate each other in the field (Mlčoch and Schulmann, 1992; Kröner et al., 1995). The tectonics of the Krušné hory Mountains is commonly interpreted as a result of a large-scale westward oriented continental collision (Matte et al., 1990). This thrusting event is documented by the presence of a flat foliation, an E–W trending lineation and commonly observed westward directed kinematics (Rajlich, 1987; Matte et al., 1990; Mlčoch and Schulmann, 1992). Recently published studies show that this thrusting was associated with the emplacement of a large-scale crustal nappe over the Saxothuringian parautochthon (Klápová et al., 1998; Krohe, 1998). The main argument for the presence of an allochthonous unit is the widespread occurrence of mafic eclogites surrounded by non-eclogitic rock assemblages (Konopásek, 1998; Rötzler et al., 1998; Klápová et al., 1998; Schmädicke et al., 1992). However, the exact boundary between the parautochthonous and allochthonous units is poorly documented. Closer examination of mapped geological structures (Hoth et al., 1994), as well as a detailed field structural survey, shows that the E–W thrusting is not the only Variscan tectonic

\* Corresponding author. Fax: +420-2-2195-2238.

E-mail address: kony@natur.cuni.cz (J. Konopásek).

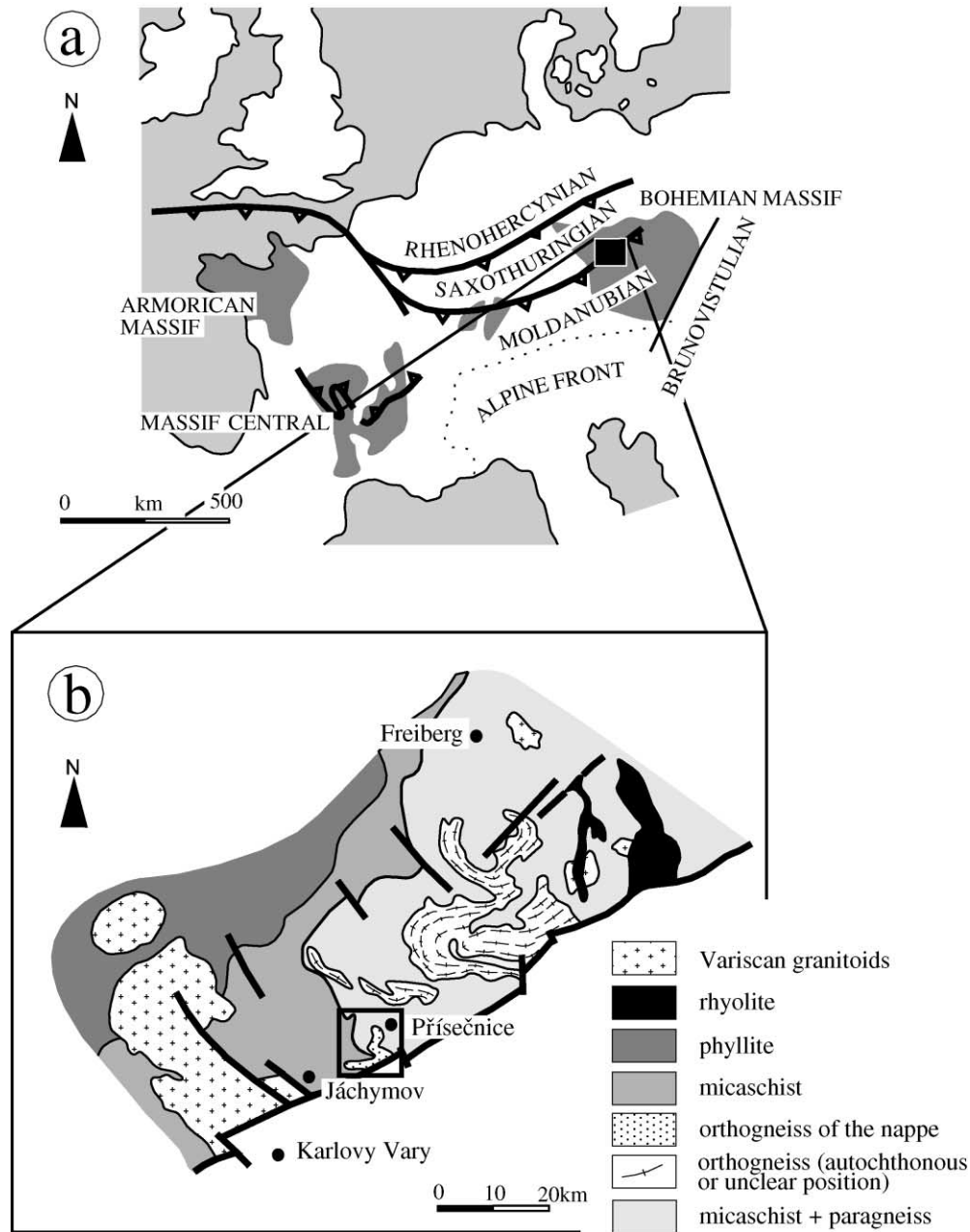


Fig. 1. (a) Location of the Krušné hory Mountains in the European Variscides (black square in the northern part of the Bohemian Massif). (b) Simplified geological map of the central part of the Krušné hory Mountains with the studied area outlined by a black line.

event responsible for the building of the final geological pattern.

In this paper we document that the structural fabric associated with emplacement of a crustal nappe is later affected by an important N–S compression, which is responsible for regional-scale refolding of a previously developed flat lying foliation. We discuss the succession of deformational events in conjunction with the thermal evolution and changing stress regimes through time. We also correlate small-scale structures and observed finite strain ellipsoids with stresses operating during the crustal-scale folding associated with exhumation of the middle crust.

## 2. Geological setting

The Bohemian Massif represents the easternmost crystalline complex of the European Variscides. Its western part is composed of the Saxothuringian domain, which has been already recognised by Kossmat (1927) as a unit with a distinct lithological and stratigraphic evolution with respect to the more easterly lying units—the Teplá–Barrandian and the Moldanubian domains.

The area studied is situated in the central part of the Krušné hory Mountains (Erzgebirge), which represent the easternmost termination of the Saxothuringian domain.

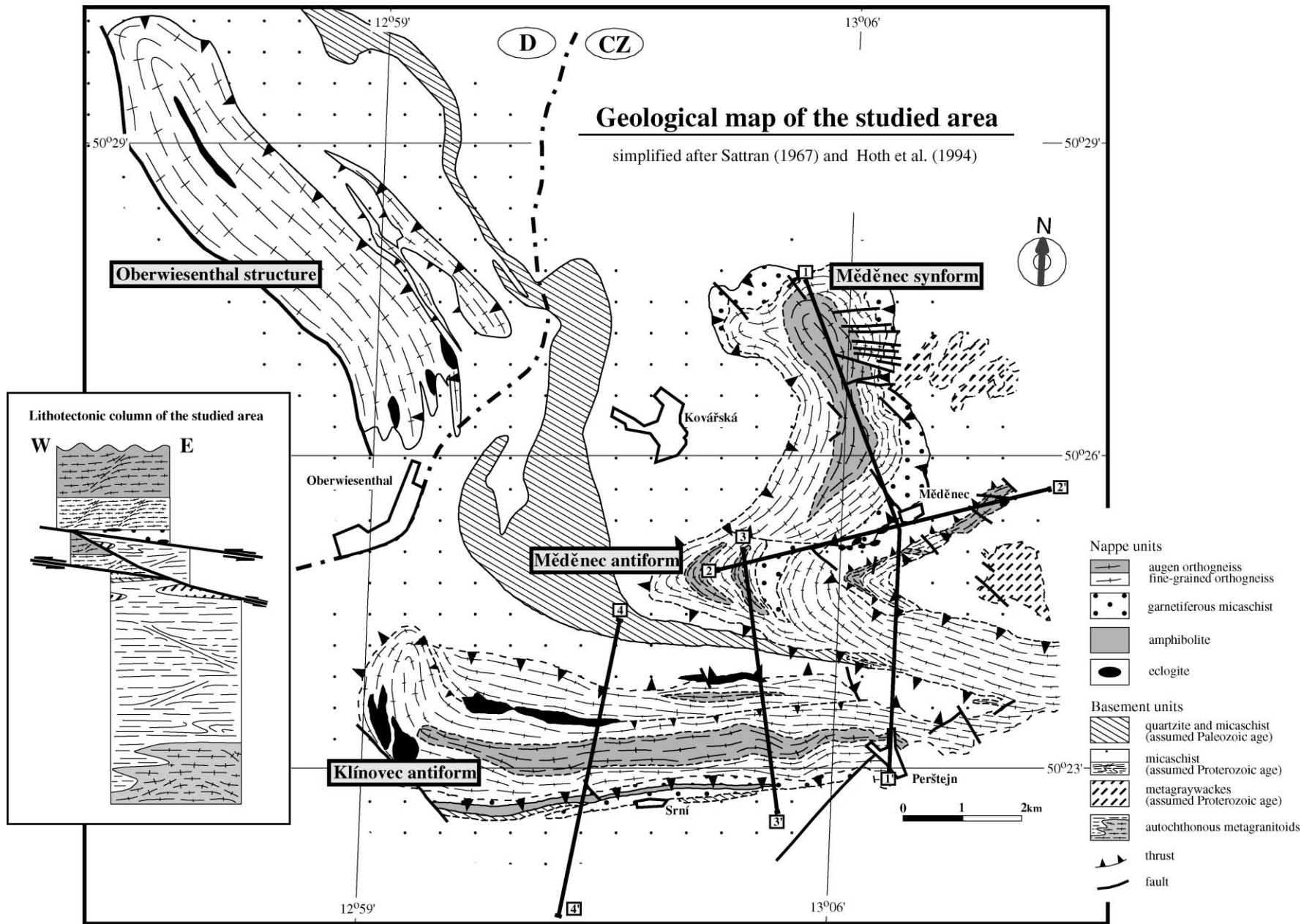


Fig. 2. Synoptic geological map of the studied area (simplified after Sattran (1967) and Hoth et al. (1994)). The inset represents lithotectonic column. Solid black lines show the position of cross-sections presented in Fig. 3.

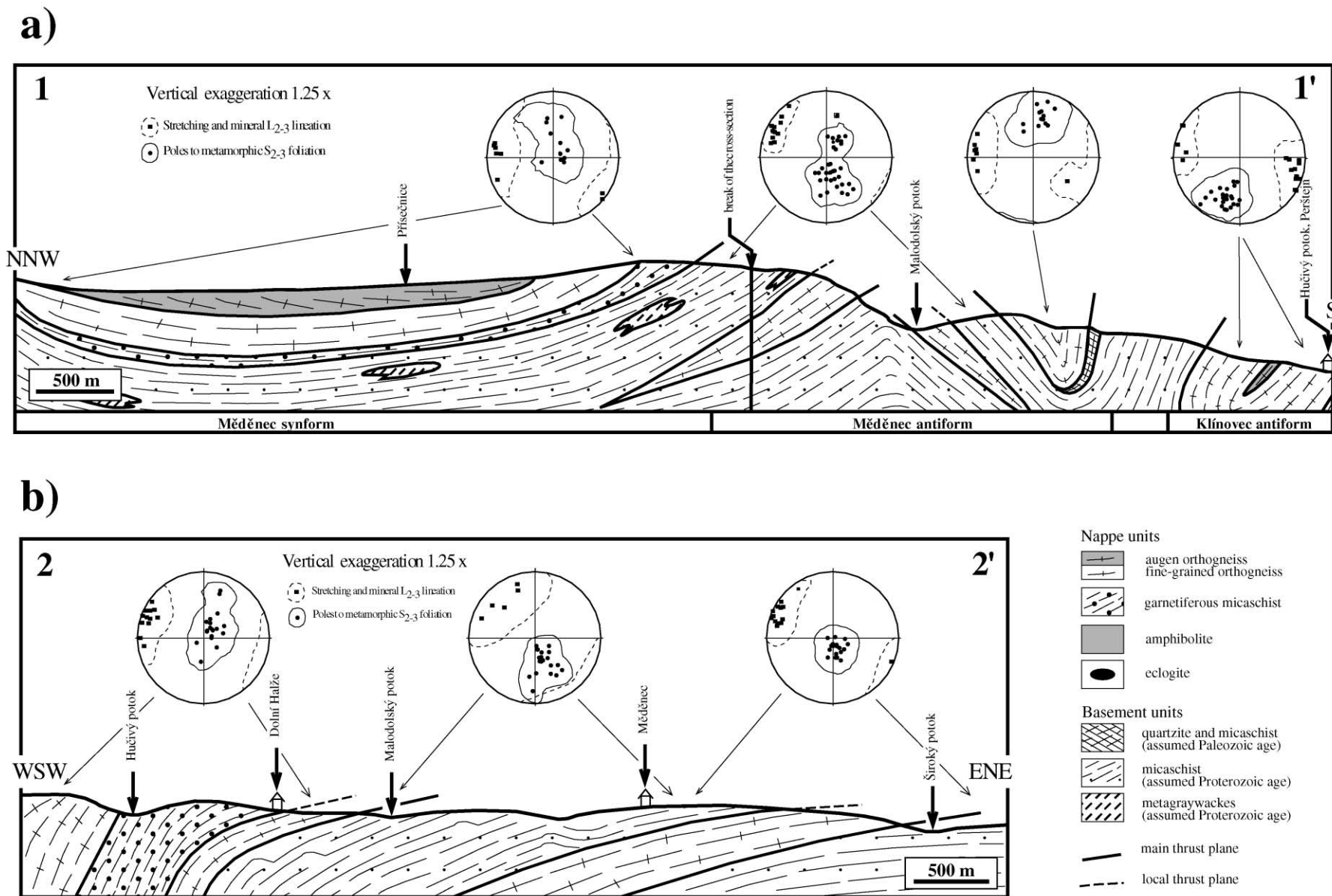


Fig. 3. (a)–(d) Cross-sections over the studied area with D2–D3 structural data represented by the lower-hemisphere equal area projection. Data are contoured at 1 × uniform distribution. See Fig. 2 for the position of cross-sections.

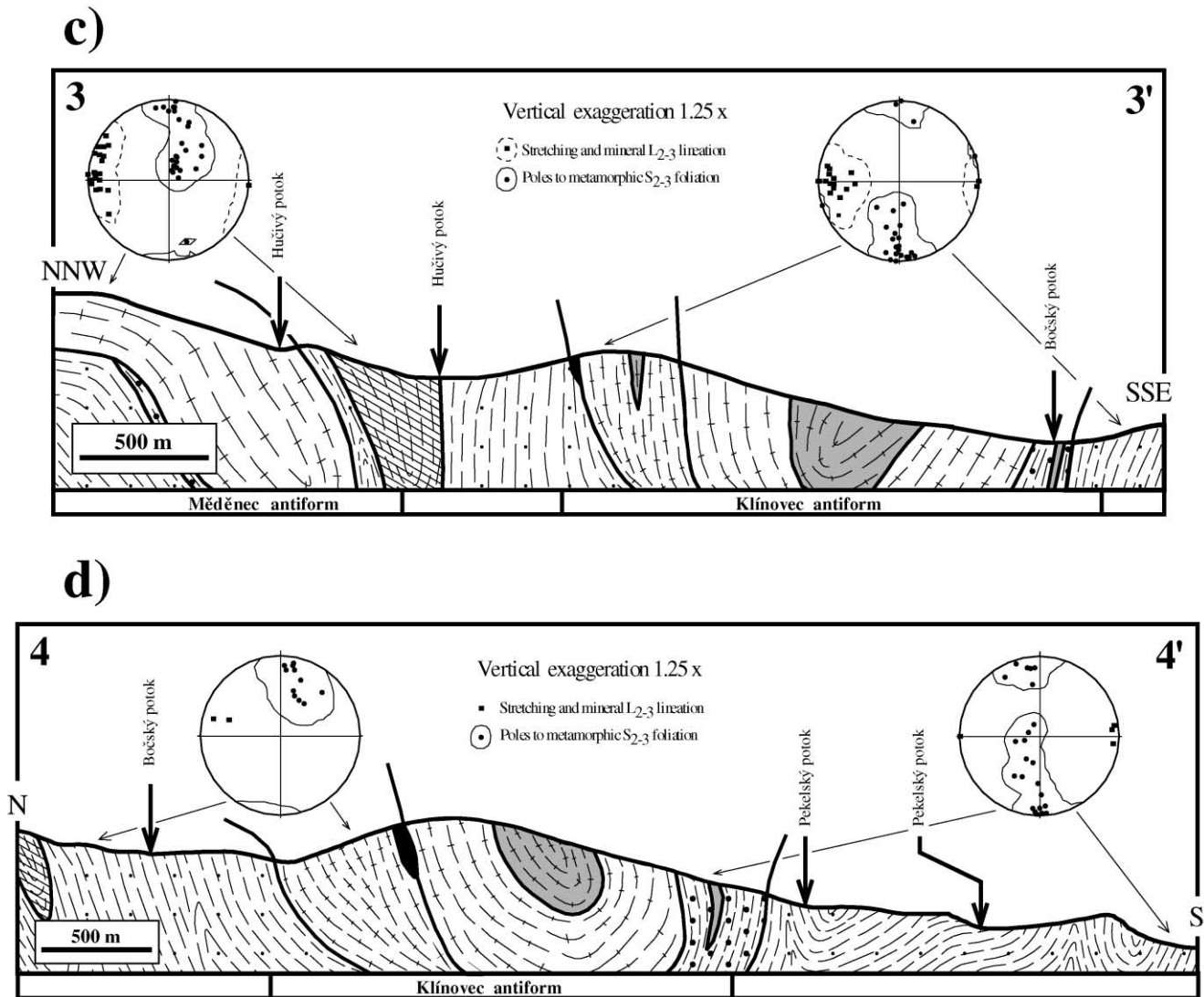


Fig. 3. (continued)

The Krušné hory Mountains form an antiform-like structure with Proterozoic metamorphic rocks in its core and with a Palaeozoic metasedimentary cover. The age of metamorphism was thought to be dominantly Variscan with decreasing metamorphic conditions from the east to the west (Kossmat, 1925) (Fig. 1).

The core of this structure is represented mainly by a monotonous complex of micaschists with subordinate meta-greywackes (the Osterzgebirge complex) and by metapelites, orthogneisses and numerous bodies of eclogites in the uppermost part (the Přísečnice complex) (Hofmann et al., 1988). The metasedimentary cover consists of quartzites, micaschists and phyllites of Lower Paleozoic age (Hoth et al., 1979). This subdivision is based exclusively on lithological arguments, however, and no structural and metamorphic features of the area were considered.

Mlčoch and Schulmann (1992) suggested a Cadomian age of metamorphism for anatectic orthogneisses in the central part of the Krušné hory Mountains, which were

intruded by a large late-Cadomian porphyritic granite. A Neo-proterozoic age for this pluton ( $554 \pm 10$  Ma—U/Pb zircon method), as well as that of surrounding migmatites, was obtained by Kröner et al. (1995). The Cadomian structure was subsequently reworked by the Variscan deformation and metamorphism that dominates in the entire area (e.g. Schmädicke et al., 1995; Kotková et al., 1996; Werner et al., 1997; Kröner and Willner, 1998).

*PT* data from all major lithologies suggest a high *dP/dT* gradient during Variscan metamorphism (Schmädicke et al., 1992; Holub and Souček, 1994; Kláková et al., 1998; Konopásek, 1998; Rötzler et al., 1998). In the German part of the Krušné hory Mountains, Willner et al. (1994) have proposed three major high-pressure (HP) units, with decreasing metamorphic grade from the lowermost to the uppermost unit. Krohe (1996) interpreted this feature as a result of ductile extension during exhumation of the thickened Saxothuringian domain. All these units contain mafic eclogites and some of them HP granulites (Willner

et al., 1997) with peak *PT* conditions differing considerably from those of the adjacent metasediments (Rötzler et al., 1998).

Metamorphic conditions in the study area are similar to those defined in Germany. A high *dP/dT* gradient was observed in metasedimentary rocks (Konopásek, 1998, 2001) which host mafic eclogites. The peak *PT* conditions of the eclogites are not consistent with those of the adjacent parautochthonous metasediments, however, suggesting that they have been juxtaposed tectonically (Klápová et al., 1998).

### 3. Lithological zonation of the studied area

The area studied involves four main large-scale structures exposed in the vicinity of the village of Měděnec—the Měděnec synform, the Oberwiesenthal structure, the Měděnec antiform and the Klínovec antiform (Škvor, 1975) (Fig. 2). These large structures are composed of the following rocks:

1. *Plagioclase schists* are described by Konopásek (1998) as characteristic metasediments forming the Saxothuringian parautochthon. Typical samples contain reversely zoned plagioclase porphyroblasts enveloping numerous garnet inclusions. As these rocks show a poly-phase metamorphic history, they can be sampled at different stages of their evolution (Konopásek, 1998). These rocks are intercalated with metagreywackes ('Dichte Gneisse' of Pietzsch (1914)) and metaconglomerates (Mehnert, 1939; Sattran, 1963).
2. *Orthogneisses* appear either as fine-grained equigranular varieties or as deformed porphyritic granite ('Rote Gneisse' of Scheumann (1935)). Porphyritic orthogneisses are heterogeneously deformed and occur in all deformation stages ranging from protomylonitic metagranites up to banded ultramylonites.
3. *Garnetiferous micaschists* are characterised by the appearance of numerous garnet porphyroblasts, sometimes up to 2 cm in diameter, surrounded by a white mica and quartz matrix. In the southern limb of the Klínovec antiform, garnetiferous micaschists are associated with a layer of *amphibolites* (Fig. 2).
4. *Mafic eclogites* bear a typical HP mineral assemblage consisting of omphacite + garnet + zoisite + amphibole + rutile + quartz and hand specimens are characterised by well-developed planar and linear fabric (Klápová et al., 1998).

The rock-types described above occur in all the large-scale structures, but the lithological zonation within these structures is not uniform. In the Měděnec synform, plagioclase schists with metagreywackes represent structurally the deepest level. These schists pass upward into the layer of garnetiferous micaschists associated with the mafic

eclogites. In the hanging wall of garnetiferous micaschist, there occurs a large slab of orthogneisses with a fine-grained variety at the bottom and a porphyritic type at the top (Fig. 3a—northern part of the profile 1–1'). Locally, fragments of the allochthonous orthogneiss slab can be observed also within the parautochthonous micaschists (Fig. 3b). The lithological zonation of the Klínovec antiform is more complicated. In its eastern part, the zonation of the southern limb is the same as that in the Měděnec synform (Fig. 3c—southern part of the profile 3–3'). However, farther to the west, the lithotectonic zonation becomes progressively reversed with orthogneisses in the lowermost position passing in the garnetiferous micaschists and with plagioclase schists in the uppermost position (Fig. 3d—southern part of the profile 4–4'). Moreover, in the core of the Klínovec antiform, large bodies of eclogites are situated in the centre of the orthogneiss body (Fig. 2).

Field observations show that mafic eclogites, together with a layer of garnetiferous micaschists, are in most cases exposed along the boundary between the orthogneisses and plagioclase schists. The location of these units along this boundary is critical for understanding the tectonic evolution of the studied area.

### 4. *PT* evolution of the studied area and the definition of the allochthonous and parautochthonous domains

The *PT* conditions of orthogneiss formation are not known, but the stability of plagioclase in all the studied samples excludes the possibility of them being deformed under eclogite facies conditions. The peak pressure conditions of the plagioclase schists were established to be 13–15 kbar at a temperature of 580–630°C (Konopásek, 1998). These pressure conditions are in contrast with those reported by Klápová et al. (1998) from the mafic eclogites where peak pressures were estimated to be 26 kbar at 650–700°C. The *PT* conditions of the associated garnetiferous micaschists approach those of the eclogites (640°C, 22 kbar—Konopásek, 2001). The difference between *PT* estimates from parautochthonous metasediments and eclogites was explained in terms of emplacement of previously subducted oceanic crust into continental rocks during the early stages of collision (Klápová et al., 1998).

As noted earlier, the mafic eclogite bodies associated with the garnetiferous micaschists occur systematically at the boundary between plagioclase schists and orthogneisses. This observation suggests that this boundary represents a major crustal boundary along which mafic eclogites were exhumed and incorporated into the middle crust. According to the interpretation of Konopásek (1998) and Klápová et al. (1998), the plagioclase schists represent a Saxothuringian parautochthon, which was overthrust by middle-crustal orthogneisses derived from an orogenic root domain, today exposed in the eastern Moldanubian zone. Based on this interpretation, these allochthonous orthogneisses,

together with mafic eclogites and garnetiferous micaschists will be referred to as the Lower Crystalline Nappe.

## 5. The succession of deformation structures (D1–D3)

A polyphase tectonic evolution has resulted in four (D1–D4) stages of deformation. The structures developed in the eclogites have been described by Klápová et al. (1998) and are, therefore, not examined in detail here, except when necessary for the interpretation of a particular deformation stage.

### 5.1. D1 structures

The D1 structures are present exclusively in the eclogites and consist of syn-metamorphic  $S_1$  foliation and an  $L_1$  lineation. As described by Klápová et al. (1998), the  $S_1$  metamorphic foliation is mainly the result of a planar orientation of omphacite and a metamorphic layering characterised by an alternation of omphacite-rich layers with layers rich in garnet. The  $L_1$  stretching lineation is characterised by a shape-preferred orientation of omphacite crystals. The orientation of D1 structures in eclogitic boudins varies according to their position within large-scale structures over the studied area (see Klápová et al. (1998) for details).

### 5.2. D2 structures

The D2 deformation in eclogites is marked by the development of asymmetric internal foliation boudinage with neck zones filled with quartz, rutile, amphibole, paragonite and zoisite. Brittle cracks up to several meters long have developed; they are either closed or filled with the same assemblage as the neck zones (Klápová et al., 1998).

The D2 structures in non-eclogitic lithologies can be best observed in the northern part of the studied area (in the Oberwiesenthal and Měděnec synforms) where the rocks are only slightly affected by the D3 deformation. Large domains of D2 fabric only slightly affected by D3 deformation also appear in the basement metasediments exposed south of the Klínovec antiform.

In the orthogneisses, the  $S_2$  foliation is characterised by the alternation of recrystallised quartz and feldspar ribbons with phyllosilicate rich domains, and in metasediments mainly by preferred orientation of micas and by alternation of mica-rich and quartz-rich layers. The orientation of the  $S_2$  foliation in the Měděnec synform is variable but it generally strikes N–S and dips gently between 10 and 20°. In the Oberwiesenthal structure, the  $S_2$  foliation is flat lying in its northern part and becomes steeply inclined as one moves south. The  $L_2$  stretching and mineral lineation is defined by an alignment of quartz and feldspar aggregates and by a stretching of quartz-rich aggregates in the orthogneisses, and as a preferred arrangement of micas in

the metasediments. The orientation of the  $L_2$  lineation is generally ESE–WNW (Fig. 4).

Numerous kinematic indicators such as sigmoidal K-feldspar porphyroclasts and  $S$ – $C$  fabrics in porphyritic orthogneiss (Fig. 5a) and shear-bands in metasediments are consistent with top-to-the-west oriented shearing. In several places, early  $F_2$  isoclinal, recumbent folds were observed in basement rocks of semipelitic composition (Fig. 5b). These early folds refold the primary compositional banding  $S_0$  of the metasediments leading to its complete transposition into a penetrative metamorphic fabric. The orientation of early  $F_2$  fold hinges is E–W, being parallel to the  $L_2$  mineral lineation (Fig. 4).

During late stages of the D2 deformation, the whole assembled sequence was folded into large-scale periclinal structures (further described as the late  $F_2$  folds) with subvertical, N–S trending axial planes. These late  $F_2$  periclinal folds form the present day Měděnec synform and the Oberwiesenthal structure.

### 5.3. D3 structures

In the southern termination of the Měděnec synform, the  $S_2$  fabric dips gently to the NW. As one moves south, the orientation of the metamorphic fabric and the lithological bodies rotate so that the foliation dips steeply to the south (Figs. 3a and 4). This geometry suggests that the gently dipping planar fabric of the Měděnec synform is refolded by the large Měděnec antiform with the hinge zone plunging to the west at a shallow angle. This fold is asymmetrical with a steeply dipping southern limb, a gently dipping northern limb and a hinge zone plunging gently to the west.

A similar pattern is developed in the Oberwiesenthal structure and the Klínovec antiform. The Oberwiesenthal structure has, in its eastern part, a similar geometry to the Měděnec synform and shows progressive decrease of the interlimb angle to the south (Fig. 4). The connection between the Oberwiesenthal synform and the Klínovec antiform is eroded and the later structure represents, as in the case of the Měděnec structures, a former N–S trending synclinal structure rotated into an E–W direction (Fig. 2). In the E–W trending limb, the foliation is subvertical (Fig. 5c) and the hinge of this large fold is steeply plunging to the SW. This is documented by the linear fabric of mafic eclogites, which plunges steeply in the same direction. The appearance of eclogite bodies in the centre of the Klínovec antiform, as well as double thickness of the fine-grained orthogneisses in the northern zone of the Klínovec antiform (Fig. 2) suggest that the northern part of this E–W trending limb was thickened during the the D2 thrusting episode.

The mineral lineation in the Oberwiesenthal structure, the Měděnec synform and the Měděnec antiform shows a uniform WNW–ESE orientation (Fig. 4), consistent with other parts of the Krušné hory Mountains parautochthon (e.g. Mlčoch and Schulmann, 1992). In the Klínovec antiform, the mineral and stretching lineation of the

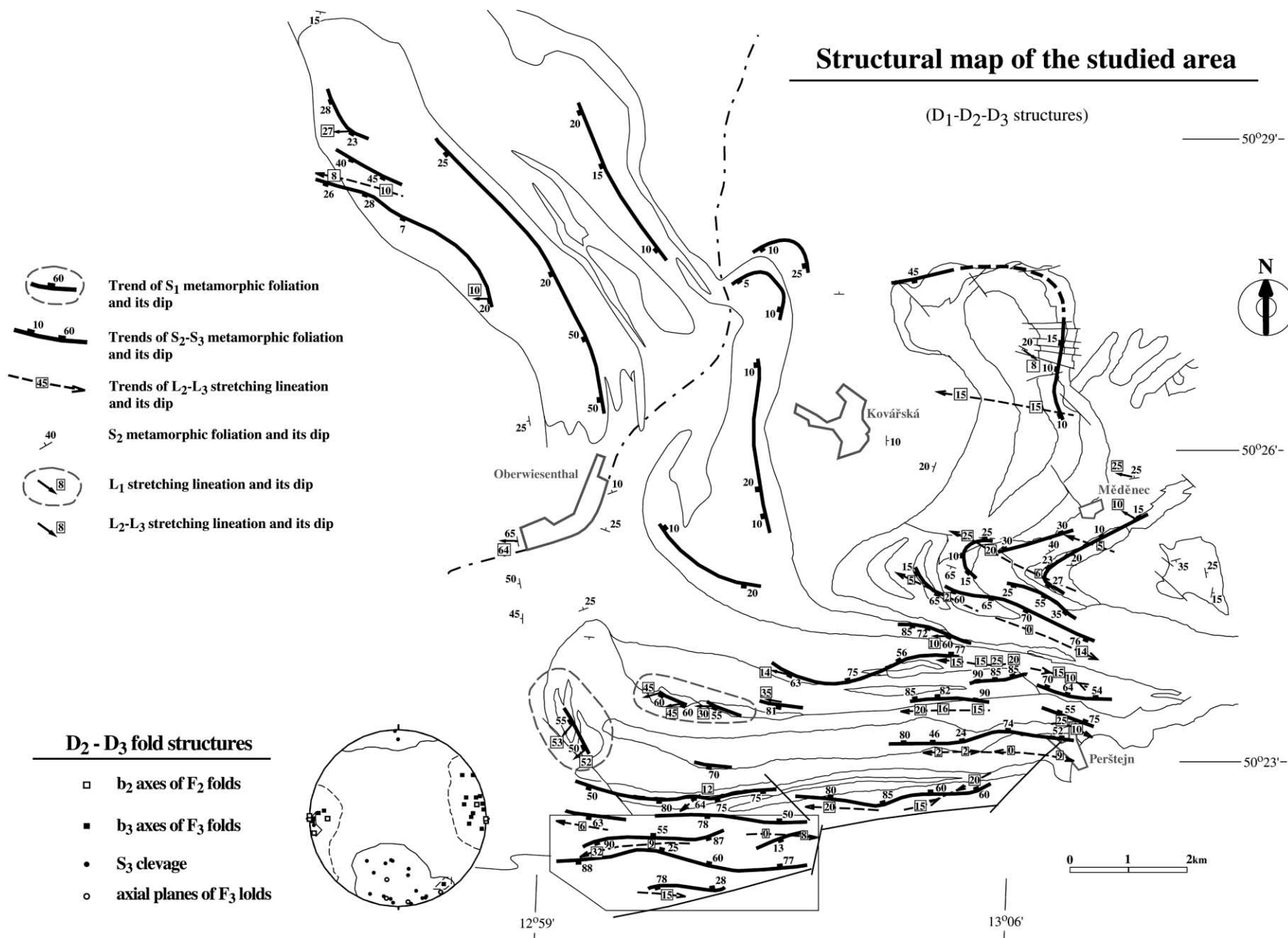


Fig. 4. Structural map of the studied area showing trends of D<sub>1</sub>, D<sub>2</sub> and D<sub>3</sub> planar and linear structures.



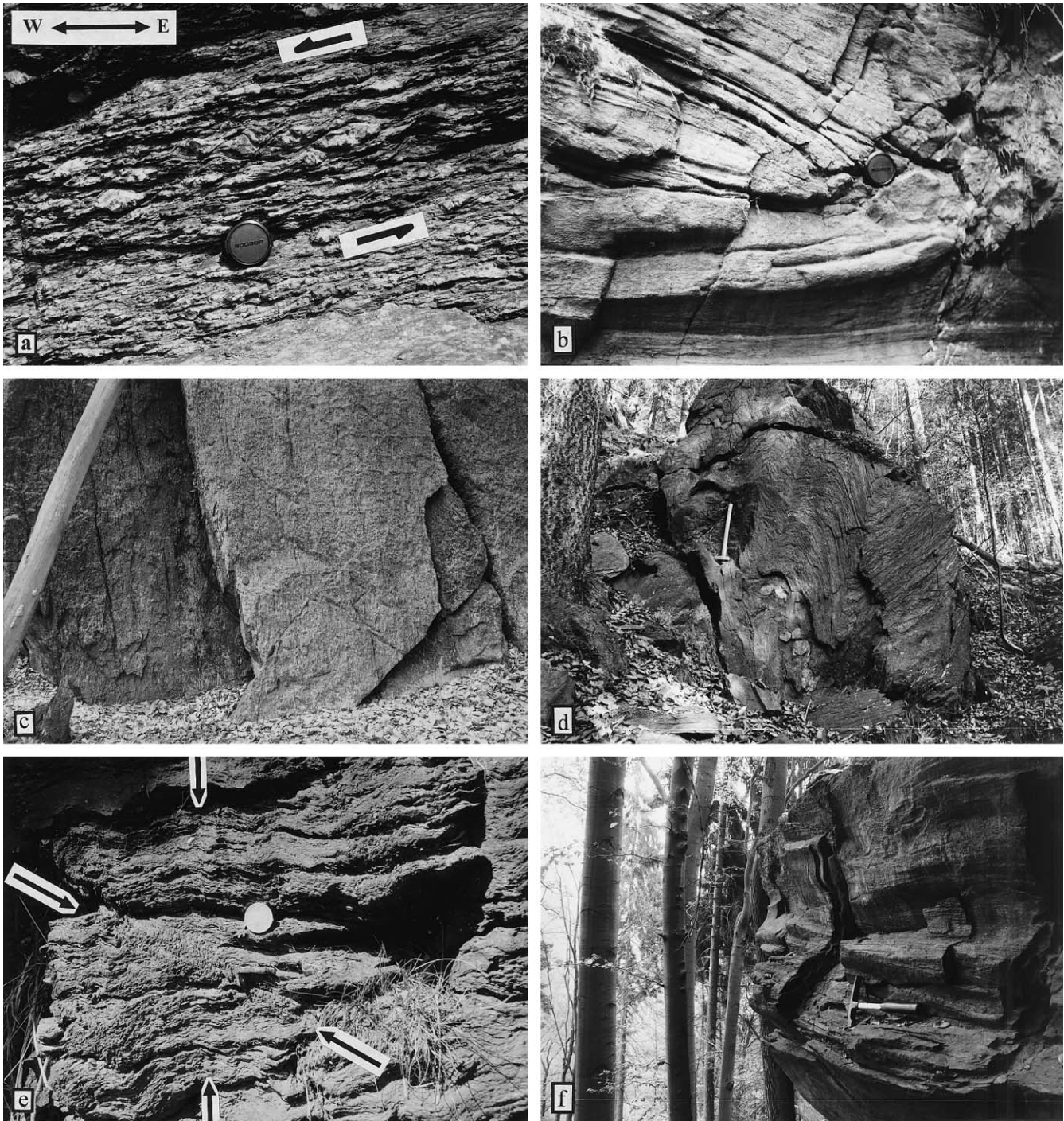


Fig. 5. (a)  $S$ - $C$  fabric in porphyritic orthogneiss of the Lower Crystalline nappe. This fabric originated during  $D2$  and suggests top-to-the-west oriented sense of movement. (b) Isoclinal  $F_2$  fold in metagreywackes of the parautochthonous unit. (c) Vertical  $S_2$  foliation in the southern limb of the Klínovec antiform. This vertical fabric resulted from refolding of originally flat  $S_2$  foliation during  $D3$ . (d)  $F_3$  fold with steep axial plane in the autochthonous plagioclase schists south of the Klínovec antiform. (e) Conjugate system of  $D3$  kink bands affecting the  $S_2$  foliation in the hinge zone of the Měděnec antiform. (f) Late  $F_4$  folds with subhorizontal axial planes in amphibolite of the southern limb of the Klínovec antiform.

orthogneisses is systematically plunging gently to the W (Fig. 4), whereas in the eclogites, the omphacite  $L_1$  lineation is gently plunging to the W-WSW in the central part of the Klínovec antiform and steeply to the SW in the hinge zone.

Numerous  $D3$  fold structures up to several metres in size with E-W trending subhorizontal hinge zones and steep to

intermediate, mostly northward dipping axial planes occur in the parautochthonous plagioclase schists south of the Klínovec antiform (Figs. 4 and 5d).

The  $D3$  deformation is most intense in the parautochthonous plagioclase schists in the area between the northern limb of the Klínovec antiform and the southern limb of

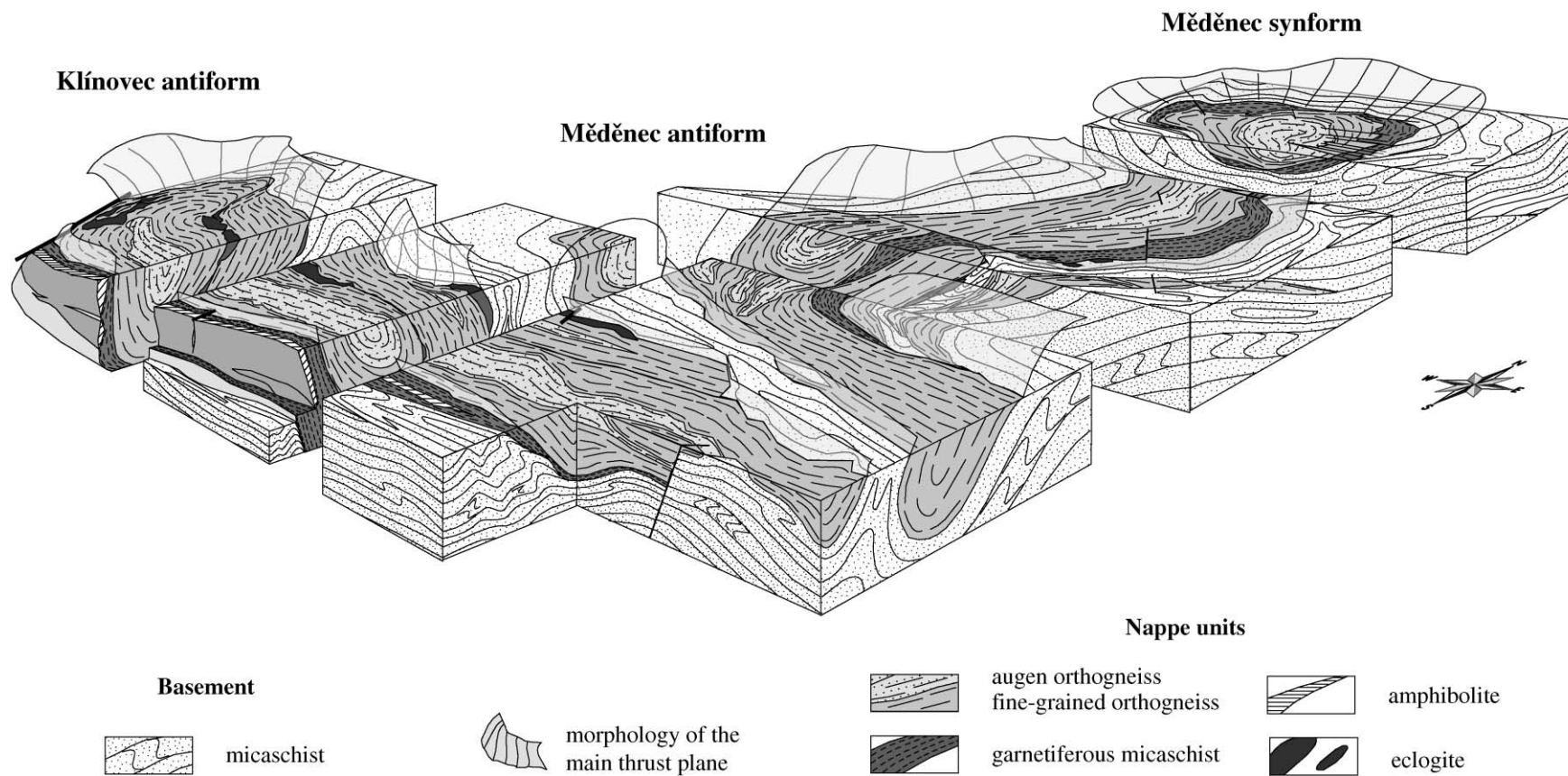


Fig. 6. Schematic block-diagram of the studied area. Flat lying  $S_2$  foliation can be observed in the northern part of the studied area in the Měděnec synform. Going to the south, the early  $D_2$  fabric is completely reworked by  $D_3$  deformation. The Oberwiesenthal structure is not shown.

the Měděnec antiform. In this area, the  $S_2$  fabric is completely reworked into a steep to subvertical E–W trending  $S_3$  foliation. Here, a strong sub-horizontal stretching of quartz aggregates can be observed in several places. In the hinge zone of the Měděnec antiform, monoclinical or conjugate kink bands are developed affecting the early  $S_2$  metamorphic foliation of the garnetiferous micaschist and orthogneisses. These kink bands exhibit E–W trending axes and kink planes, bimodally distributed with respect to flat-lying  $S_2$  foliation (Fig. 5e). The geometry of these kink bands suggests that they are genetically linked to the Měděnec antiformal D3 structure but the mechanism and the kinematics of kinking will be discussed in a separate section below.

The general structure of the studied domain is shown in block-diagram (Fig. 6), summarising lithological and structural observations discussed above as an effect of the D3 folding superimposed on the D2 fabrics.

## 6. Problem of the $L_2$ and $L_3$ lineation solved using aggregate-shape analysis

An important feature is the parallelism of the  $L_2$  mineral lineation in the Měděnec synform (a D2 structure) with the lineation observed in micaschists and orthogneisses of both the Měděnec and the Klínovec antiforms. If the WNW–ESE trending  $L_2$  lineation in the Měděnec synform were rotated by late  $F_2$  folding, the originally EW trending, gently plunging  $L_2$  lineation would become subvertical (Fig. 7). This can be observed in N–S trending, steep  $S_2$  foliation in the southern part of the Oberwiesenthal structure. Subse-

quent rotation of the  $S_2$  foliation by  $F_3$  folds with a steep hinge zone will keep the orientation of the  $L_2$  in a subvertical position (Fig. 7). The lineation in the steep limbs of the Klínovec and the Měděnec antiforms is always found to plunge gently to the west, however, indicating that it was formed during the D3 deformation ( $L_3$  lineation). Consequently, the change of the  $L_2$  into an  $L_3$  lineation must be associated with complete modification of the D2 fabric during the D3 deformation. In order to investigate the proposed changes to the D2 fabric ellipsoid during the D3 deformation, we have carried out a shape analysis of mineral aggregates in the orthogneisses from the Měděnec synform and the Měděnec and the Klínovec antiforms.

In order to determine the role of the  $F_3$  folding in possible fabric modifications, an aggregate-shape analysis of K-feldspar and quartz was carried out on the porphyritic orthogneisses. Selected porphyritic augen orthogneisses were sampled in the hinge zones and limbs of both the Měděnec and the Klínovec antiforms, as well as in the Měděnec synform and the Oberwiesenthal structure. Two sections in each sample were studied: (a) perpendicular to metamorphic foliation and parallel to mineral lineation (the XZ section of the finite strain ellipsoid), and (b) perpendicular to both foliation and lineation (the YZ section of the finite strain ellipsoid). The shapes of the K-feldspar and quartz aggregates were traced on transparent sheet, digitised and then analysed. Because of the large size of measured aggregates, only a limited number of measurements could be carried out on each sample (Table 1). Finite strain ratios were calculated from the two principal strain ellipsoid planes using a harmonic mean method (Lisle, 1977; Ramsay and Huber, 1983, p. 80). These ratios were

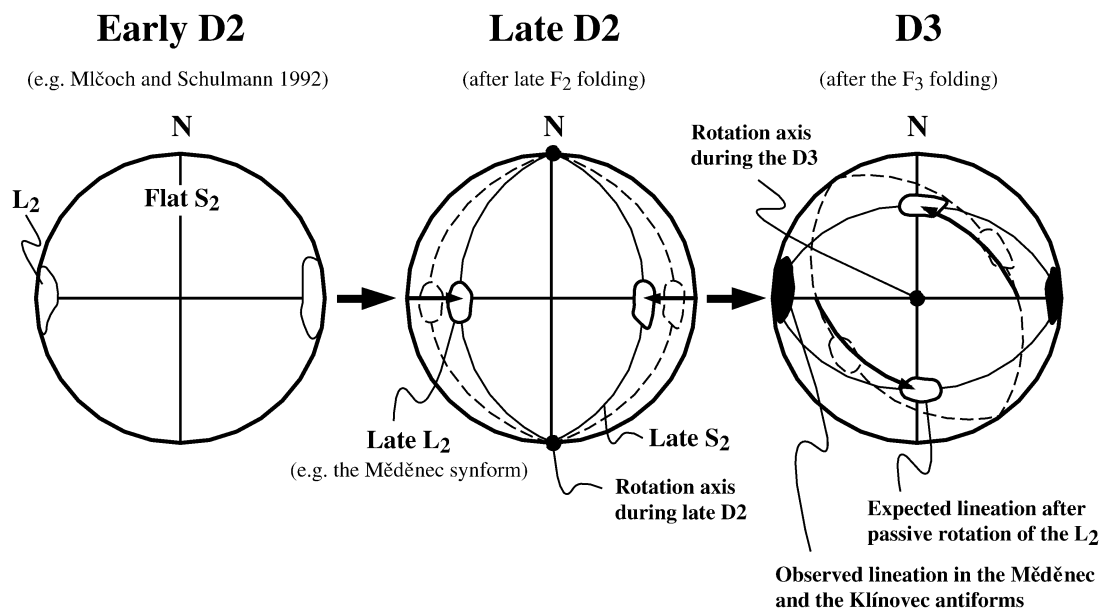


Fig. 7. Succession of the lower-hemisphere equal area projections shows schematically expected evolution of the orientation of the  $L_2$  lineation during D2 and D3 folding. Early  $L_2$  lineation is trending E–W being subhorizontal. During late  $F_2$  folding, the  $L_2$  lineation does not change the orientation, but becomes steeper. The successive  $F_3$  folding changes the orientation of steep  $S_2$  foliation; the  $L_2$  lineation should rotate into N–S direction maintaining its steep plunge. In the D3 structures (the Měděnec and the Klínovec antiforms), however, the lineation is always E–W oriented and mostly subhorizontal.

Table 1

Harmonic means of measured  $X/Z$  and  $Y/Z$  ratios and corresponding calculated  $X/Y$  ratios and  $k$  and  $d$  values for orthogneiss samples from the D2 domains (the Měděnec synform and the Oberwiesenthal structure) and the D3 domains (the Klínovec and Měděnec antiforms). See Fig. 8 for corresponding Flinn's graph and the  $d/k$  plot

Sample	Locality	Object	$X/Z$	$Y/Z$	$X/Y$	$k$	$d$	Number of objects measured:	
								in $XZ$	in $YZ$
D2									
MR10	Měděnec synform	Qtz	5.907	2.26	2.614	1.28	2.047	18	25
		Kf	3.438	1.372	2.507	4.055	1.552	4	7
MR7	Měděnec synform	Qtz	4.914	1.865	2.634	1.888	1.849	24	35
		Kf	2.525	1.831	1.379	0.456	0.914	8	16
MR8	Měděnec synform	Qtz	4.594	2.34	1.963	0.719	1.65	22	21
		Kf	1.752	1.285	1.364	1.276	0.462	7	4
OW407	Oberwiesenthal str.	Qtz	3.614	3.033	1.192	0.094	2.042	11	9
		Kf	3.794	2.234	1.699	0.566	1.418	12	14
OW417	Oberwiesenthal str.	Kf	3.891	2.372	1.64	0.466	1.514	13	13
D3									
MR115	Klínovec antiform	Qtz	5.271	2.955	1.783	0.401	2.106	10	9
		Kf	3.171	1.913	1.657	0.72	1.125	10	8
MR11	Měděnec antiform	Kf	4.209	2.488	1.692	0.465	1.641	21	49
MR12	Měděnec antiform	Kf	10.45	9.001	1.161	0.02	8.002	20	23
MR3	Klínovec antiform	Qtz	10.26	6.301	1.628	0.118	5.338	23	13
		Kf	5.487	3.194	1.718	0.327	2.309	15	11
MR401	Klínovec antiform	Qtz	12.33	8.385	1.47	0.064	7.399	10	14
		Kf	6.961	5.168	1.347	0.083	4.182	12	13

used to construct the  $k$ -parameter of Flinn (1962) and  $d$ -parameter (e.g. Ramsay and Huber, 1983, p. 202) to estimate the shape of the strain ellipsoid and strain intensity, respectively.

The finite strain analysis shows that the augen orthogneisses in the Měděnec synform, as well as those in the hinge zone of the Měděnec antiform, exhibit ellipsoids ranging from constrictional to plane-strain or slightly oblate symmetry, ( $k$ -parameters vary from 0.72 to 1.89 for quartz and 0.46 to 4.06 for feldspars—Fig. 8 and Table 1). Exceptionally oblate fabric was observed for quartz aggregates in the sample OW407 ( $k = 0.094$ ). Quartz generally shows higher strain intensity ( $d$ -parameters from 1.65 to 2) than feldspar ( $d$ -parameters from 0.9 to 1.55). In studied samples, the orthogneisses have a character of augen orthogneiss with well preserved K-feldspar porphyroclasts. In the southern, steep limb of the Měděnec antiform, and in the orthogneiss bodies of the Klínovec antiform, the shapes of strain ellipsoids are oblate ( $k = 0.4–0.06$  for quartz and  $k = 0.72–0.02$  for K-feldspar—Fig. 8 and Table 1). As in the previous case, quartz generally shows higher strain intensity ( $d$ -parameter is from 2.1 to 7.4) than feldspar ( $d$ -parameter from 1.1 to 8). The increase of deformation intensity is connected with the disappearance of augen structure and development of banded orthogneiss. It is noted that samples with weak oblate symmetry show well-developed  $L_3$  lineation characterised by stretching of feldspar and quartz aggregates. In contrast, samples with strong oblate symmetry do not show any stretching lineation and the  $L_3$  fabric is characterised only by alignment of white mica in the foliation plane.

We suggest (in agreement with the mesoscopic structural data) that the symmetry of the D2 deformation is represented by a plane strain to constrictional or slightly oblate strain ellipsoid resulting from westward directed non-coaxial shearing. This symmetry is preserved in both the Měděnec synform and the Oberwiesenthal structure and probably also in the hinge zone of the Měděnec antiform. In contrast, the shapes of K-feldspar and quartz aggregates in the limbs of the Klínovec antiform show oblate geometry, high strain intensity and  $X$ -axes oriented E–W. As mentioned above, this type of geometry cannot be produced by passive rotation of the D2 fabric during the  $F_3$  folding and we propose that the large-scale  $F_3$  folding is responsible for the modification of the shapes of the D2 strain ellipsoid. The aggregate shape analysis also shows that the large scale  $F_3$  folding occurred under still elevated thermal conditions, which allowed ductile deformation of feldspar clasts.

## 7. Brittle-ductile structures (late D3 and D4)

As reported by Klápová et al. (1998), the D4 deformation in the eclogites resulted in the development of two main sets of structures. Most frequently, the D4 deformation produces late  $S_4$  retrograde shear zones, which crosscut the  $S_1$  eclogitic foliation at high angles. In the thick eclogite boudins, the D4 deformation has resulted in the refolding of the early  $S_1$  foliation. There, D4 structures are open to closed recumbent, asymmetrical  $F_4$  folds. The D4 deformation is best recorded in amphibolites, garnetiferous micaschists and basement plagioclase schists, and is

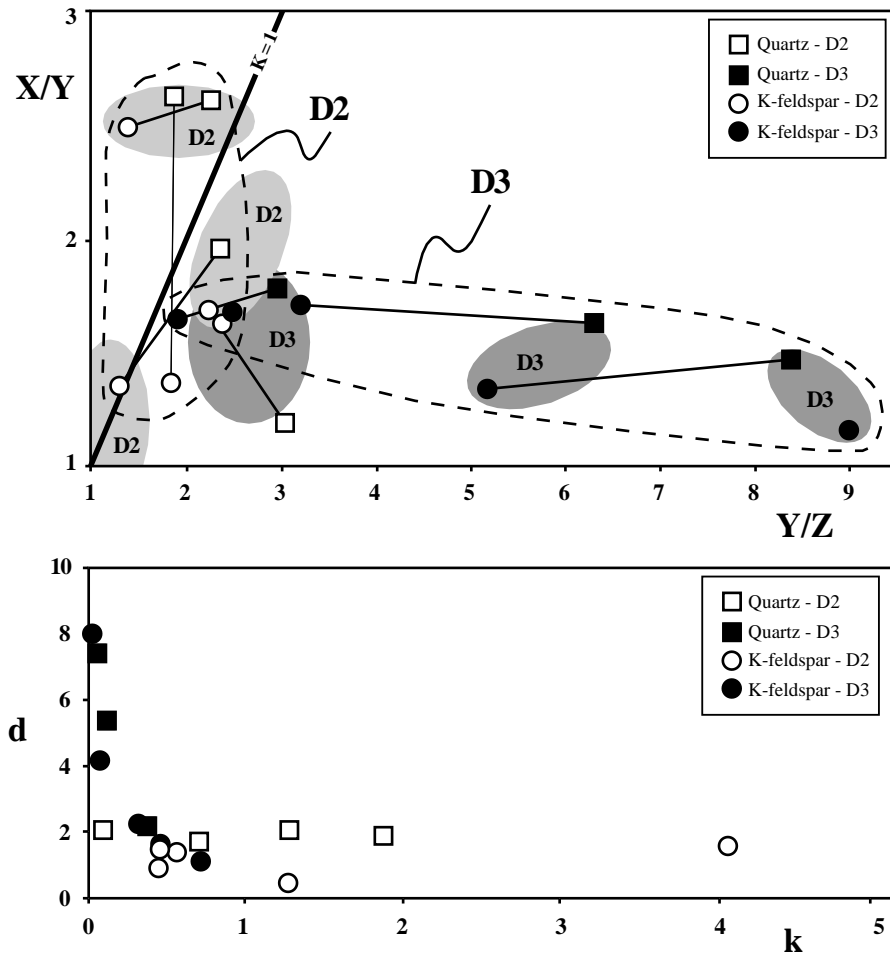


Fig. 8. Flinn's graph and  $d/k$  plot obtained from measurements of K-feldspar and quartz aggregates in coarse-grained orthogneisses of the Měděnec nappe. In the Měděnec synform and northern part of the Měděnec antiform (D2 structures), both K-feldspar and quartz aggregates show plane strain to prolate symmetry at relatively low strain intensities. On the other hand, the same aggregates in the southern limb of the Měděnec antiform and in the Klínovec antiform (D3 structures) show oblate symmetry and higher strain intensities (see text for methods and details). Grey areas represent starting and ending positions of the D2 ellipsoids used for modelling of the D3 fabric. Results of this modelling are presented in Fig. 10.

represented by late  $F_4$  folds and kink bands (Fig. 5f). The latest deformation in the metasediments is represented by semi-brittle normal faults dipping to the SW. These occur on the southern limb of the Klínovec antiform. Evidence of the D4 deformation in orthogneisses is rare. The D4 structures appear mostly in the southern limb of the Klínovec antiform as discrete sets of brittle-ductile  $S_4$  cleavage with homogeneous spacing obliquely oriented to the main  $S_2$  foliation (Fig. 9).

#### 7.1. The D3 and D4 kink-band folds in metasediments and orthogneisses

In several places, conjugate arrays of kink-band folds were observed, but in most cases only one single set is developed (monoclinical kink-band folds after Ramsay and Huber (1987), p. 427). All these kink-band folds are of contractional type (Ramsay and Huber, 1987, p. 427) and their common feature is an E–W orientation of their hinges.

In the northern limb of the Měděnec antiform (close to the hinge zone, Fig. 9) several localities with well-developed kink-band folds occur. These appear in both the metasediments and the orthogneisses in zones where the  $S_2$  fabric dips gently (Loc. 130, 130.V, 6, 138—Fig. 9). The same type of kink-band folds can be locally observed in zones of flat lying  $S_2$  metamorphic fabric south of the Klínovec antiform (Loc. 307). These kink-band folds, which are either conjugate or form a single set with a uniform orientation of the kink-plane, are related to the D3 deformation.

The D4 kink-band folds are developed exclusively in zones of steep  $S_2$ – $S_3$  fabric in both the plagioclase schists and the garnetiferous micaschists, and are most frequently observed in close proximity to the allochthonous orthogneiss body. Three groups of D4 kink-band folds are recognised and these are shown in Fig. 9. A group (a) is made up from a set of monoclinical kink-band folds, which affect foliations dipping steeply to the north. They indicate top-to-the-north normal movement. Group (b) consists of

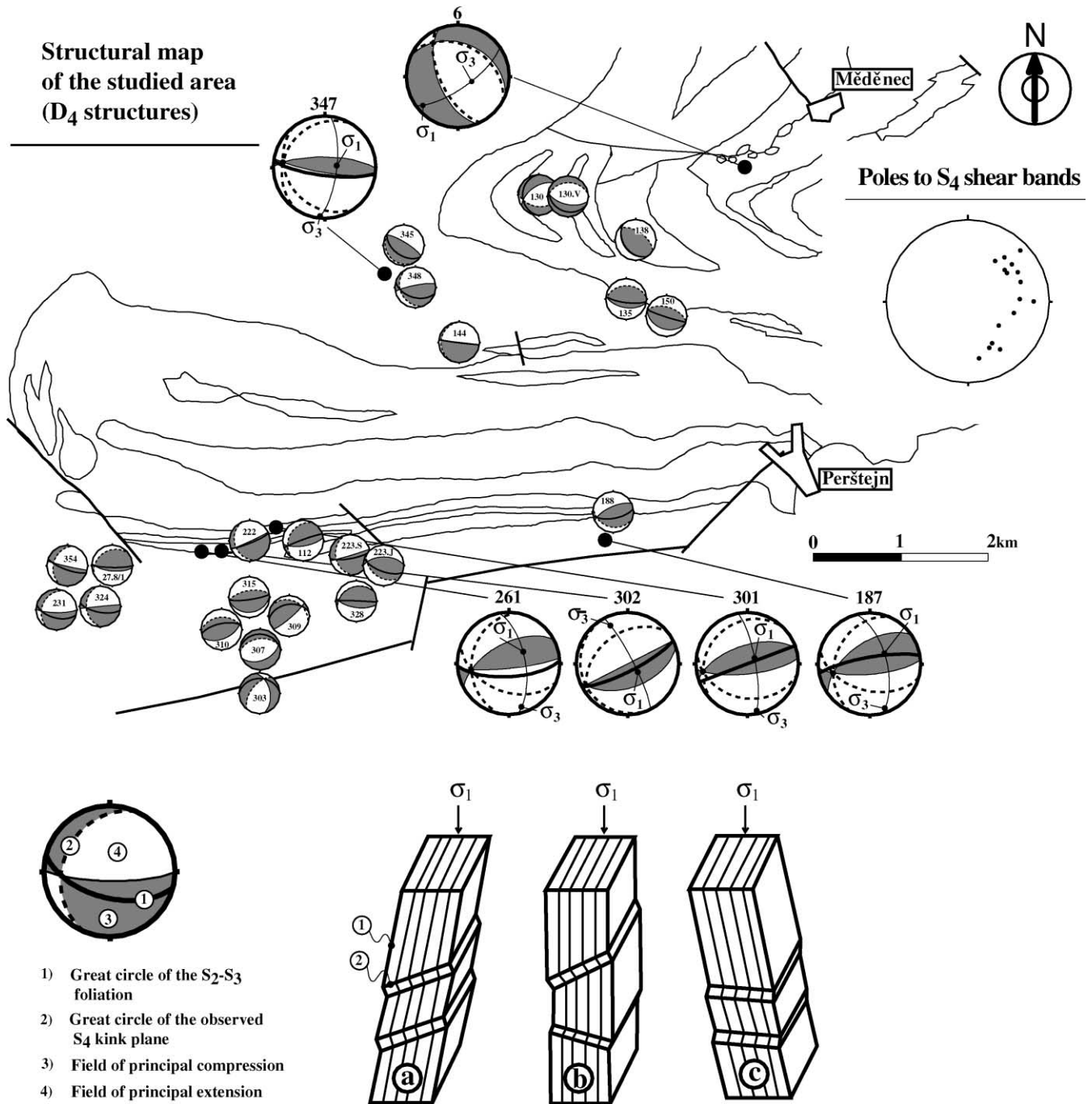


Fig. 9. Structural map of the studied area shows D<sub>3</sub> and D<sub>4</sub> monoclinial and conjugate systems of kink bands. Orientation of the kink bands is presented in the lower-hemisphere equal area projection together with the orientation of S<sub>2</sub>–S<sub>3</sub> foliation (see lower left part of the figure for principal fabric elements). For each locality (numbered inside or above each projection), all measured kink bands and foliations were averaged and presented as a mean value. Estimated  $\sigma_1$  and  $\sigma_3$  directions are shown at localities with developed conjugate kink bands. The equal area projection on the right hand side of the figure represents poles to brittle-ductile, late D<sub>4</sub> shear bands in orthogneisses and micaschists. Three groups of F<sub>4</sub> compressional kink bands observed in the studied area are shown in the lower part of the figure. (a) Kink bands showing northward normal kinematics affecting northward dipping steep foliation. (b) Conjugate set of kink bands affecting subvertical foliation. (c) Kink bands showing southward normal kinematics affecting southward dipping steep foliation.

symmetrically developed conjugate kink-band folds and these are developed in a vertical foliation. Group (c) consists of monoclinial kink-band folds which deform a steep, south-dipping foliations and indicates top-to-the-south normal kinematics.

In the southern limb of the Klínovec antiform, most of the kink-band folds belong to group 3, with groups 2 and 1 observed less frequently. On the southern limb of the Měděnec antiform, the three groups of kink-band folds are more equally developed.

## 7.2. Analysis of kink-band folds

The geometry of symmetrical kink-band folds was used to determine the orientation of stress axes according to the method of Ramsay (1962a). The orientation of  $\sigma_1$  is perpendicular to the kink-band fold axis and lies in the plane that bisects the obtuse angle between the conjugate kink-band folds. If only one set of the conjugate kink-band folds develops, it implies that the maximum principal compressive stress  $\sigma_1$  was oblique to the foliation. The approximate orientation can be deduced but, as the angle between  $\sigma_1$  and the kink-band fold is determined by the value of the mechanical anisotropy (Cobbold et al., 1971) and because of the phenomenon of stress deflection, it is not possible to determine the exact orientation of  $\sigma_1$ .

The sub-horizontal orientation of  $\sigma_1$ , deduced from the geometry and orientation of the D3 kink-band folds, is consistent with earlier deduced N–S compression associated with the D3 deformation. Some of them show signs of later rotation, which probably occurred during the progressive development of the D3 folding (e.g. Locality 6 in Fig. 9).

The uniform orientation of the D4 fold axes and the essentially bimodal distribution of kink-band folds in the southern limb of the Klínovec antiform (Fig. 9) indicate that they probably represent a conjugate set (groups (a) and (c), Fig. 9). This conjugate set is developed throughout the whole study area. Locally, only one set of the kink-band folds is found to have developed and, as discussed above, this can be interpreted as a result of variations of the  $S_2$ – $S_3$  orientation with respect to principal compression. The stress analysis of both the monoclinic and conjugate kink-band folds shows that the principal compression  $\sigma_1$  during the D4 deformation was subvertical.

## 8. Discussion

### 8.1. Kinematic interpretation of the D1–D2 structural succession—building of the nappe pile

The D1 fabric in eclogites has developed during a pressure and temperature peak in spatially different setting than the present-day country rocks. After their emplacement in the crust, the eclogites were passively transported at the base of the Lower Crystalline Nappe during the D2 thrusting and behaved as rigid inclusions in a weak matrix of micaschists. This kind of behaviour resulted in the non-uniform orientation of the D1 structures within the isolated eclogitic boudins which were developed mainly during the large-scale D3 folding (Klápová et al., 1998).

The D2 structures in the parautochthonous plagioclase schists, and in the allochthonous orthogneisses, are associated with the main metamorphic event. They represent syn-metamorphic structures developed during the westward thrusting of the Lower Crystalline Nappe over

the metasedimentary Saxothuringian parautochthon, as inferred from numerous kinematic indicators. Klápová et al. (1998) suggested that the D2 structures in the eclogites developed in the same kinematic regime.

During the final stages of D2, the principal compression that was acting E–W caused large-scale buckling of the whole nappe sequence and of the parautochthonous domain. These buckle folds have vertical axial planes and fold hinges perpendicular to the  $L_2$  stretching lineation. We interpret these structures as a result of the buckling of the stacked nappe sequence at the end of a D2 thrusting episode caused by the buttressing effect of a rigid autochthon. The Měděnec synform and the Oberwiesenthal structure originated in the same manner.

### 8.2. F3 refolding and regional interference pattern

Two large-scale  $F_3$  antiforms later refolded the whole nappe system, together with the parautochthonous sequence. These antiforms have E–W striking steep axial planes and westward plunging hinge zones. In the Klínovec antiform, the D3 deformation is associated with the rotation of the omphacite  $L_1$  lineation in the eclogites as a result of the active rotation of eclogitic boudins within weaker orthogneisses and metasediments.

The increase in the intensity of the D3 folding in the south of the study area may be the result of the original geometry of the D2 synforms. If the late  $F_2$  folds have a large wavelength and small amplitude (as, for example, the Měděnec synform), later compression parallel to their axes will result in the development of dome and basin structures (interference pattern type I of Ramsay (1962b)). The observed structural pattern indicates, however, that late  $F_2$  folds are overprinted by  $F_3$  folds with moderate to steeply plunging hinges. The development of this kind of  $F_3$  fold suggests that late  $F_2$  folds were non-cylindrical domes and basins elongated in a N–S direction with increasing amplitude to the south. Such periclinal basins and domes are commonly described from the Zagros Mountains (Iran) or the Jura Mountains (Price and Cosgrove, 1990, pp. 262–263). The N–S compression of such a structure may produce the observed large folds with steeply plunging hinges and E–W vertical axial plane. In this manner, an interference pattern of type II originates (Ramsay, 1962b). The D3 folding intensity is thus controlled by D2 fold shape with basement depth increasing towards the south and interlimb angle increasing towards the north.

### 8.3. Strain pattern in the $F_3$ fold limbs and $F_3$ fold mechanics

The strain ellipsoid in the limb zones of both the Klínovec and Měděnec antiforms is characterised by oblate shapes suggesting flattening perpendicular to the  $F_3$  fold axial plane (Fig. 8). Moreover, the X-axis of finite strain in these zones is sub-horizontal and E–W in direction as a result of the D3 deformation. We suppose that in E–W

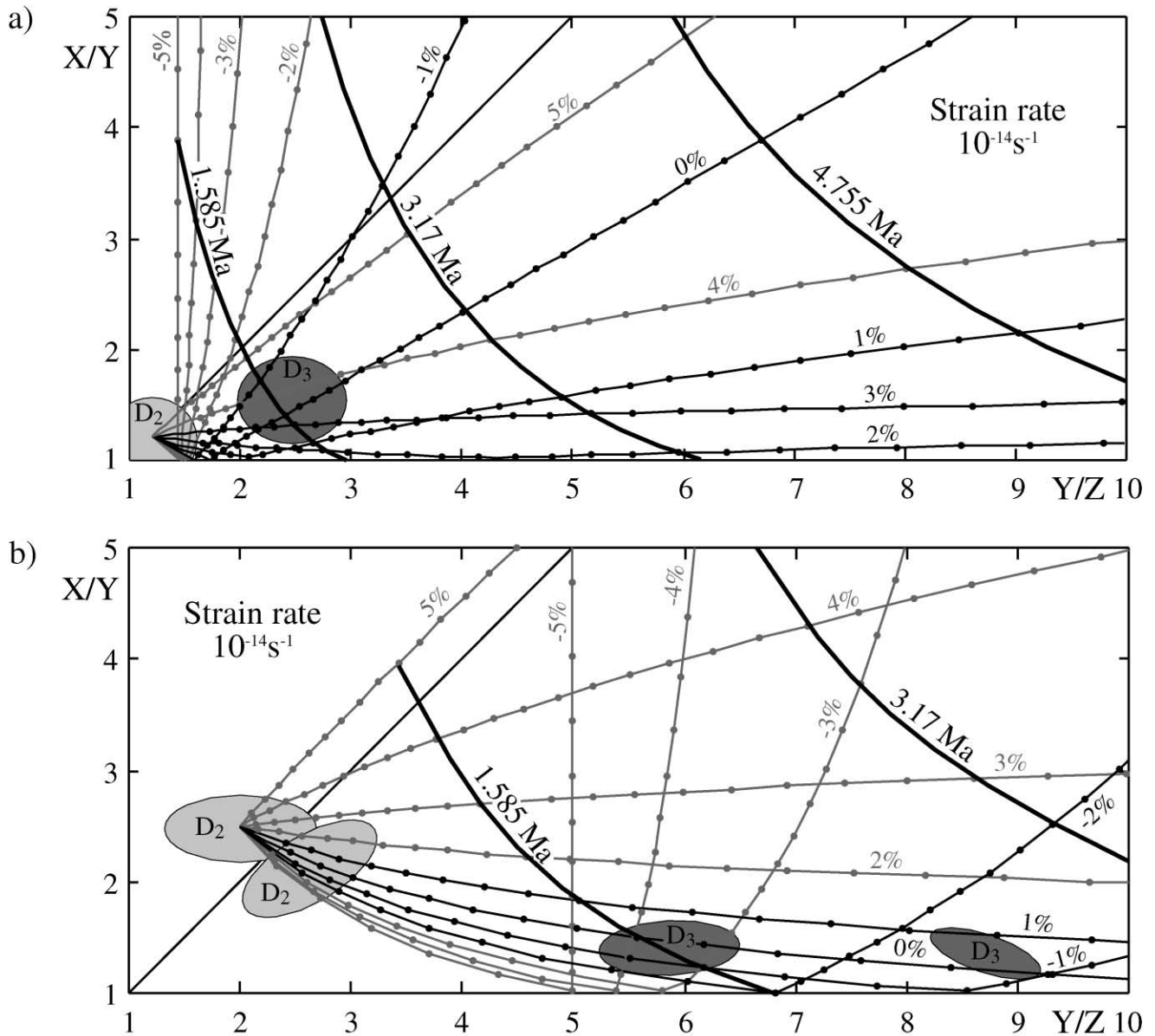


Fig. 10. Calculated evolution of the D3 fabric as a result of homogeneous isovolumic pure-shear deformation applied to the D2 strain ellipsoid with N–S trending Z-axis and vertical X-axis. Black and grey lines show the evolution of the strain ellipsoid with 5% step of strain (black dots) being labeled by percent of strain accommodated by the X-axis of the D2 strain ellipsoid (negative values represent shortening). (a) Results of calculation starting from the D2 ellipsoid with the plane strain symmetry and low strain intensity (grey field labeled D2). Provided that almost the entire D3 deformation is accommodated by the E–W trending Y-axis of the D2 ellipsoid, after 40–50% of shortening by pure-shear, the resulting fabric will show E–W trending long axis, oblate symmetry, and still relatively low intensity of deformation (grey field labeled D3). (b) Results of calculation starting from the D2 ellipsoid with prolate symmetry and medium intensity of deformation (grey field labeled D2). Provided that almost the entire D3 deformation is accommodated by the E–W trending Y-axis of the D2 ellipsoid, after 40–60% of shortening by pure-shear, the resulting fabric will show weak vertical elongation, oblate symmetry and high strain intensity (grey field labelled D3).

oriented limbs, the ductile shortening was superimposed on the original D2 plane strain fabric.

We have simulated superposition of homogeneous coaxial deformation on a plane-strain ellipsoid with steep X-axis and vertical E–W trending XY plane (D2 fabric after  $F_3$  passive folding—Fig. 7) and the results are shown in Fig. 10. From the above presented geological arguments, it is assumed that the D2 and D3 Z-axes were parallel

after rotation of  $S_2$  foliation during large scale  $F_3$  folding. Thus, considered isovolumic changes of the shape of fabric ellipsoid are induced by shortening of the former Z-axis. This isovolumetric strain is accommodated by differential elongation of former Y- and X-axes of the D2 ellipsoid. Paths in Fig. 10 represent different amounts of elongation of the former X-axis (negative values represent shortening). Points on the strain paths



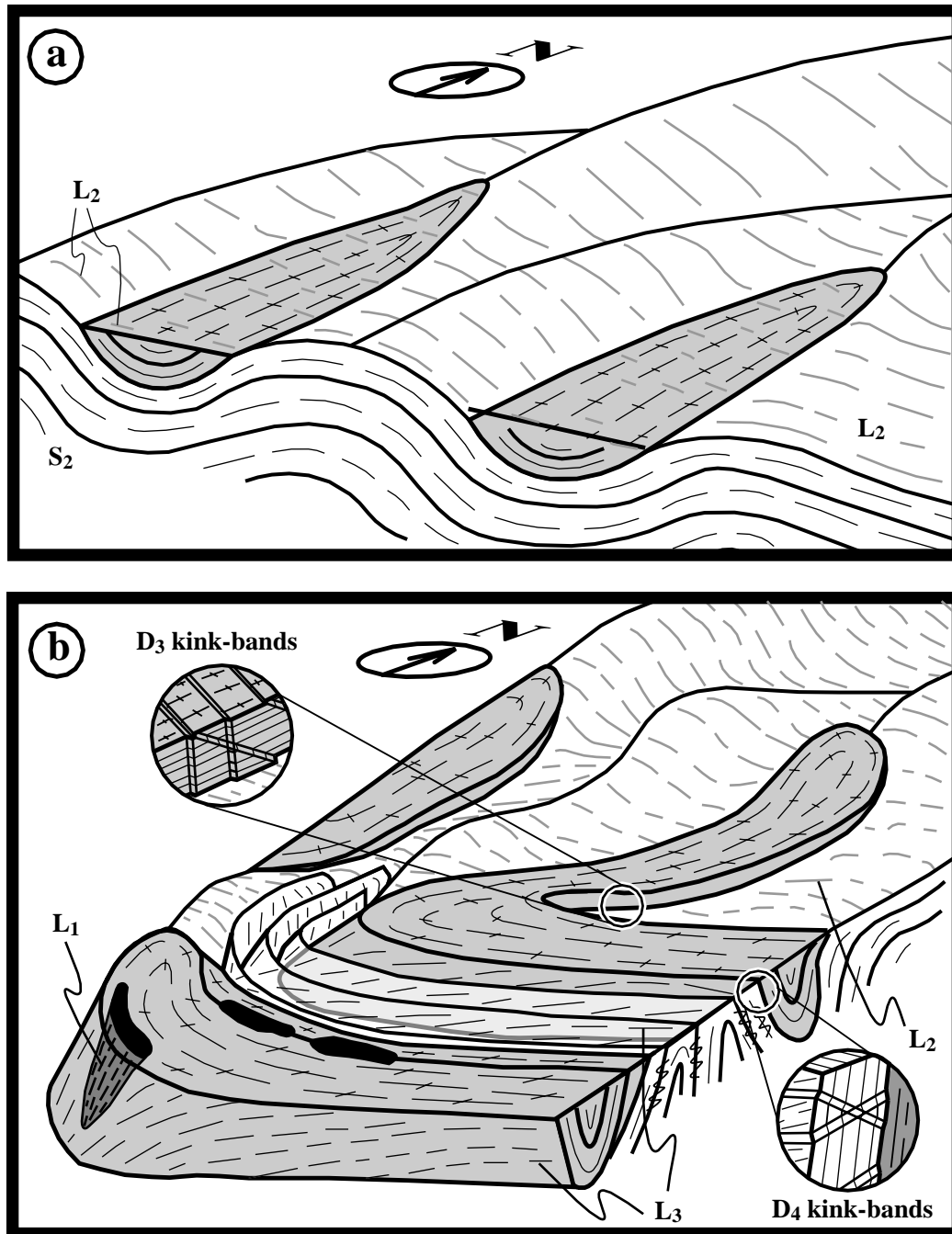


Fig. 11. Schematic sketches showing the evolution of large-scale structures in time. (a) Situation after the late D2 deformation is interpreted as a result of buttressing of the allochthonous unit from the west. Continuous E–W compression leads to the development of large-scale periclinal structures (the Měděnec synform and Oberwiesenthal structure). (b) Subsequent N–S compression leads to refolding of the late D2 structures by km-scale antiforms (the Měděnec and Klínovec antiforms). Brittle-ductile structures in the flat lying S<sub>2</sub> foliation appear during the late D3 deformation. Disappearance of the N–S oriented D3 compressive stress leads to strengthening of the role of overburden. Vertical D4 compression produces D4 kink-band folds to kink-bands.

show 5% increments of strain imposed on a former D2 fabric ellipsoid.

In those areas that were not affected by the D3 deformation, we have identified three types of the D2 strains symmetries (Fig. 8) and these approximately represent starting points of trajectories in the Fig. 10. An attempt was made to find those finite strains observed in natural samples from the

megafold limbs. Moreover, different finite D3 fabrics must be produced after an equal number of increments of the D3 deformation. Our analysis demonstrates (Fig. 10) that this case is reached when most of the imposed shortening is accommodated by elongation of former Y-axis and small change of former X-axis. For plane-strain to constrictional vertical D2 fabric with higher strain intensity (Fig. 10a),

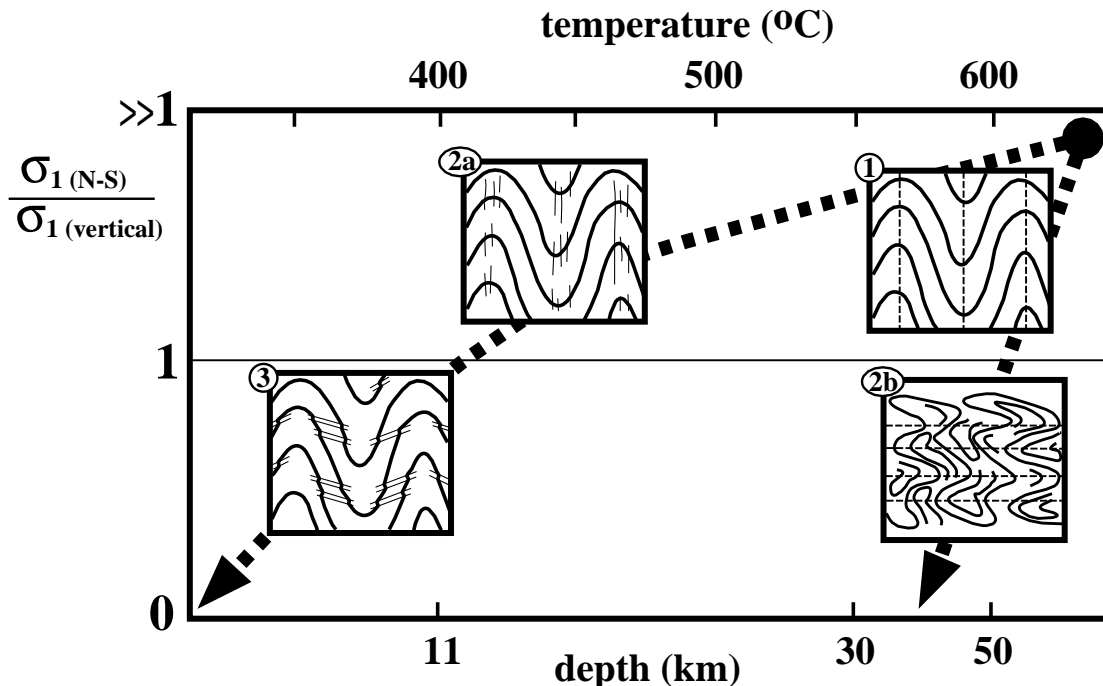


Fig. 12. Diagram of the orientation of  $\sigma_1$  versus depth and temperature during D3 and D4 shows two possible scenarios of such an evolution. Path 1–2a–3 shows N–S compression during exhumation of the studied area, which is demonstrated by progressive development of brittle-ductile D3 structures. After the decreasing role of the N–S compression at shallow crustal levels and low temperature, the prevailing vertical compression will produce the D4 kink-bands. This scenario is consistent with field observations. The path 1–2b shows the diminishing role of the N–S compressive stress and increase in the importance of vertical compression caused by the overburden at high temperatures in depth. This evolution would result in refolding of the  $F_3$  folds by ductile  $F_4$  folds with subhorizontal axial planes. The *PT* path adopted from Konopásek (2001).

superimposed D3 deformation will produce strong oblate fabrics without macroscopically visible aggregate lineation. In the case of low D2 strain intensities (Fig. 10b), the resulting fabric is marked by L–S symmetry with intermediate intensities and visible horizontal  $L_3$  aggregate stretching lineation (former *Y*-axis).

The field observations suggest that the  $F_3$  folds developed by mechanisms of buckling of a single layer of orthogneiss surrounded by micaschist. Strong flattening in the limb areas of the Klínovec antiform also indicates conditions of moderate viscosity contrast between strong orthogneisses and weak micaschists.

#### 8.4. The origin of the D3–D4 kink bands and other D4 brittle-ductile structures

A question arises: were the above-described D4 kink-bands developed as post-D3 structures, or were they created during the early D3 deformation and then re-oriented during the D3 folding? As described above, the steep metamorphic fabric in metasediments between the northern limb of the Klínovec antiform and the Měděnec antiform, as well as the zone of metasediments in the southern limb of the Klínovec antiform, are believed to represent the  $S_3$  cleavage. Therefore, the kink-bands affecting the  $S_3$  cleavage must be post-D3. This is the case of those kink-folds developed in the steep southern limb of the Měděnec antiform and in the

steep zones south of the Klínovec antiform. On the other hand, the kink-bands developed in the hinge zone of the Měděnec antiform actually correspond to the axial cleavage of this structure and are, therefore, developed in the early stages of D3 folding.

If we accept a hypothesis that the kink-bands in metasediments close to the Klínovec and the Měděnec antiforms were not generated in the same stress field as the D3 large scale folds, another local source of stress must have existed to generate these structures. A possible source of stress during the D4 is the weight of the overburden after the relaxation of the D3 stresses. This will produce subvertical  $\sigma_1$ , which has been documented in the southern part of the Klínovec antiform. Moreover, the expected deformation associated with the relaxation of the D3 stresses is rather low. This is consistent with the development of kink bands and brittle-ductile cleavage in orthogneisses and metasediments. The amount of strain achieved during their development is probably more than two orders of magnitude less than the deformation associated with the D1–D3 deformation and, thus, rather insignificant at the scale of the studied area.

#### 8.5. Variations of principal compression direction through time

The analysis of the D2, D3 and D4 structures shows

complex stress–temperature–time evolution (Fig. 11). As discussed above, the D2 structures are associated with westward thrusting of the Lower Crystalline nappe over the Saxothuringian basement suggesting non-coaxial deformation with E–W oriented  $\sigma_1$  direction.

Strain analysis within D3 fold limbs indicates a N–S oriented horizontal compression  $\sigma_1$  and important vertical stress  $\sigma_2$  inhibiting elongation in the vertical direction. Then, the only elongation accommodating N–S horizontal compression  $\sigma_1$  is possible in the horizontal E–W direction. This indicates an important role of rigid overburden for stresses acting in a low viscosity layer at depth. Sub-horizontal N–S compression leads to lateral flow of material without the vertical component in the early stages of D3 deformation. The same stress regime, however, is responsible for the formation of kink band structures in the hinge of the Měděnec antiform. Kink band structures represent a brittle-ductile regime (Dewey, 1965, 1969) and, thus, indicate a decrease in temperature under the same orientation of the D3 stress field. It is, therefore, suggested that the horizontal N–S compression operated during an uplift of the whole region from the deep to the supracrustal level.

The presence of D4 kink bands must be associated with the disappearance of horizontal stresses and increase in subvertical  $\sigma_1$  compression. If this change of stress regime would occur at high temperature conditions, then the  $F_3$  folds would be refolded by large-scale ductile  $F_4$  folds with subhorizontal axial planes. Fig. 12 documents that the  $F_3$  folding started at peak temperature conditions (ca. 600°C) enabling viscous buckling of the nappe sequence caused by shortening in the N–S direction. This deformation phase continued during a temperature decrease associated with uplift, resulting in the development of D3 kink-bands and a crenulation cleavage in the hinge zones of large-scale anticlines. The latest  $F_4$  phase occurred under relatively low temperature conditions and indicates the disappearance of horizontal stress, allowing vertical shortening of steep D3 fabric. These changes in stress can be interpreted as an increase of the role of overburden after termination of the D3 compressive stress.

#### 8.6. Exhumation of eclogites and the importance of extension in the Czech part of the Krušné hory (Erzgebirge) Mountains

In contrast with the western Saxothuringian domain, where the boundary between eclogites-bearing nappes and supracrustal autochthon can be easily identified, a similar limit is difficult to establish in the eastern Krušné hory Mountains. Using structural and petrological criteria, we have defined the boundary between the parautochthonous Saxothuringian metasediments and allochthonous eclogites-bearing nappe. Thrusting-associated structures developed in both the parautochthonous and allochthonous units document that the nappe emplacement occurred in the middle crust at a

depth corresponding to 13–15 kbar. Field observations, however, are not able to provide any information about the mechanism of emplacement of eclogites from a depth corresponding to 26 kbar to the base of non-eclogitic orthogneiss nappe. This work shows mechanical behaviour of the crust during and after the nappe emplacement with eclogites as a part of lithological assemblage. The exhumation of assembled parautochthonous and allochthonous units to supracrustal levels is associated with complex structural reworking of originally simple fabric during the subsequent N–S shortening, which is responsible for the final pattern of the central part of the Krušné hory Mountains in the Czech Republic.

There is a range of publications emphasising the role of the late Variscan extensional deformation for the final tectonic and metamorphic pattern of the German part of the eastern Saxothuringian domain (Willner et al., 1994; Krohe, 1996, 1998; Rötzler et al., 1998). These interpretations are based on regional distribution of metamorphic units and orientation of shear structures in different areas of the Erzgebirge. In this study, we have examined a particularly suitable area with steeply developed anisotropy affected by vertical shortening and demonstrated that it achieves no more than first percents of the bulk strain during this event. If the extensional tectonics would be a key regime responsible for final geometry of studied crystalline complexes then significantly more important vertical shortening should be expected first in areas with subvertically developed anisotropy. Therefore, we suggest that the structural pattern of the whole Saxothuringian domain should be re-evaluated in terms of detailed structural analysis to demonstrate the real significance of late orogenic extension in this part of the Bohemian Massif.

#### Acknowledgements

We are very grateful to John Cosgrove for helpful comments on an early version of the manuscript. The paper has also benefited from the comments of G. Oliver and W. Franke. We also thank Jaroslav Synek for drawing Fig. 6. This work was funded by the Grant Agency of the Czech Republic, grant no. 205/96/0279.

#### References

- Cobbold, P.R., Cosgrove, J.W., Summers, J.M., 1971. Development of internal structures in deformed anisotropic rocks. *Tectonophysics* 12 (1), 23–53.
- Dewey, J.F., 1965. Nature and origin of kink-bands. *Tectonophysics* 1, 459–494.
- Dewey, J.F., 1969. The origin and development of kink bands in a foliated body. *Geological Journal* 6, 193–216.
- Flinn, D., 1962. On folding during three dimensional progressive deformation. *Quarterly Journal of the Geological Society of London* 118, 385–428.
- Franke, W., 1993. The Saxonian Granulites: a metamorphic core complex? *Geologische Rundschau* 82, 505–515.

- Franke, W., Dallmeyer, D., Weber, K., 1995. Geodynamic evolution (of the Variscan Belt). In: Dallmeyer, D., Franke, W., Weber, K. (Eds.). *Pre-Permian Geology of Central and Eastern Europe*. Springer-Verlag, New York, pp. 579–593.
- Hofmann, J., Mathé, G., Werner, C.D., 1988. Saxothuringian zone and the central German crystalline zone in the German Democratic Republik. In: Zoubek, V., Cogné, J., Kozhoukharov, D., Krätner, H.G. (Eds.). *Precambrian in Younger Fold Belts*. Wiley and Sons, Chichester, p. 885.
- Holub, F.V., Souček, J., 1994. Blueschist-greenschist metamorphism of metabasites in the western Krušné hory (Erzgebirge) Mts. *Zentralblatt für Geologie und Paläontologie. Teil I* 1992 (7/8), 815–826.
- Hoth, K., Lorenz, W., Hirschmann, G., Berger, H.-J., 1979. Lithostratigraphische gliederungsmöglichkeiten des regionalmetamorphen Jungproterozoikums am Beispiel des Erzgebirges. *Zeitschrift für Geologische Wissenschaften* 7, 397–404.
- Hoth, K., Wasternack, J., Berger, H.-J., Breiter, K., Mlčoch, B., Schovánek, P., 1994. *Geologische Karte Erzgebirge/Vogtland, 1:100,000*. Sächsisches Landesamt für Umwelt und Geologie.
- Klápová, H., Konopásek, J., Schulmann, K., 1998. Eclogites from the Czech part of the Erzgebirge: multi-stage metamorphic and structural evolution. *Journal of the Geological Society of London* 155, 567–583.
- Konopásek, J., 1998. Formation and destabilization of the high pressure assemblage garnet–phengite–paragonite (Krušné hory Mountains, Bohemian Massif): the significance of the Tschermak substitution in the metamorphism of pelitic rocks. *Lithos* 42, 269–284.
- Konopásek, J., 2001. Eclogitic micaschists in the central part of the Krušné hory Mountains (Bohemian Massif). *European Journal of Mineralogy* 13, 1.
- Kossmat, F., 1925. *Übersicht der Geologie von Sachsen*. G.A. Kaufmann, Leipzig.
- Kossmat, F., 1927. Gliederung des varistischen Gebirgsbaues. *Abhandlungen des Sächsischen Geologischen Landesamtes* 1, 39.
- Kotková, J., Kröner, A., Todt, W., Fiala, J., 1996. Zircon dating of North Bohemian granulites, Czech Republic: further evidence for the Lower Carboniferous high-pressure event in the Bohemian Massif. *Geologische Rundschau* 85, 154–161.
- Krohe, A., 1996. Variscan tectonics of Central Europe: postaccretionary intraplate deformation of weak continental lithosphere. *Tectonics* 15, 1364–1388.
- Krohe, A., 1998. Extending a thickened crustal bulge: toward a new geodynamic evolution model of the paleozoic NW Bohemian Massif, German Continental Deep Drilling site (SE Germany). *Earth-Science Reviews* 44, 95–145.
- Kröner, A., Willner, A.P., Hegner, E., Frischbutter, A., Hofmann, J., Bergner, R., 1995. Latest Precambrian zircon ages, Nd isotopic systematics and *PT* evolution of granitoid orthogneisses of the Erzgebirge, Saxony and Czech Republic. *Geologische Rundschau* 84, 437–456.
- Kröner, A., Willner, A.P., 1998. Time of formation and peak of Variscan HP–HT metamorphism of quartz-feldspar rocks in the central Erzgebirge, Saxony, Germany. *Contributions to Mineralogy and Petrology* 132, 1–20.
- Lisle, R.J., 1977. Estimation of tectonic strain ratio from the mean shape of deformed elliptical markers. *Geologie en Mijnbouw* 56, 140–144.
- Matte, P., Maluski, H., Rajlich, P., Franke, W., 1990. Terrane boundaries in the Bohemian Massif: result of large-scale Variscan shearing. *Tectonophysics* 177, 151–170.
- Mehnert, K.R., 1939. Die Meta-Konglomerate des Wiesenthaler Gneiszuges im sächsischen Erzgebirge. *Mineralogische und Petrographische Mitteilungen* 50, 194–272.
- Mlčoch, B., Schulmann, K., 1992. Superposition of Variscan ductile shear deformation on pre-Variscan mantled gneiss structure (Catherine dome, Erzgebirge, Bohemian Massif). *Geologische Rundschau* 81 (2), 501–513.
- Pietzsch, K., 1914. Über das Alter der dichten Gneise des sächsischen Erzgebirges. *Zentralblatt für Mineralogie* 1914, 202–211, 225–241.
- Price, N.J., Cosgrove, J.W., 1990. *Analysis of Geological Structures*. Cambridge University Press, Cambridge (Reprinted 1994).
- Rajlich, P., 1987. Hercynian ductile tectonics in the Bohemian Massif. *Geologische Rundschau* 76 (3), 755–786.
- Ramsay, J.G., 1962a. The geometry of conjugate fold systems. *Geological Magazine* 99, 516–526.
- Ramsay, J.G., 1962b. Interference patterns produced by the superposition of folds of similar types. *Journal of Geology* 70, 466–481.
- Ramsay, J.G., Huber, M.I., 1983. *The Techniques of Modern Structural Geology. Volume 1, Strain Analysis*. Academic Press, London.
- Ramsay, J.G., Huber, M.I., 1987. *The Techniques of Modern Structural Geology. Volume 2, Folds and Fractures*. Academic Press, London (Fourth printing 1993).
- Rötzler, K., Schumacher, R., Maresch, W., Willner, A., 1998. Characterization and geodynamic implications of contrasting metamorphic evolution in juxtaposed high-pressure units of the Western Erzgebirge (Saxony, Germany). *European Journal of Mineralogy* 10, 261–280.
- Satran, V., 1963. Metaconglomerates from the Krušné hory Mountains and their genetic significance. *Sborník Geologické Věd, Geologie* 2, 41–62 (in Czech).
- Satran, V., 1967. Geological map of the central part of the Krušné hory Mountains between Klášterec nad Ohří and Vejprty (1:25,000). Czech Geological Survey. Unpublished.
- Scheumann, K.H., 1935. Die Rotgneise der Glimmerschieferdecke des sächsischen Granulitgebirges. *Berichten mathematische-physikalische Klasse der sächsischen Akademie der Wissenschaften* 87, 251–286.
- Schmädicke, E., Okrusch, M., Schmidt, W., 1992. Eclogite-facies rocks in the Saxonian Erzgebirge, Germany: high pressure metamorphism under contrasting *P–T* conditions. *Contributions to Mineralogy and Petrology* 110, 226–241.
- Schmädicke, E., Mezger, K., Cosca, M.A., Okrusch, M., 1995. Variscan Sm–Nd and Ar–Ar ages of eclogite facies rocks from the Erzgebirge, Bohemian Massif. *Journal of Metamorphic Geology* 13, 537–552.
- Škvor, V., 1975. *Geology of the Czech part of the Krušné hory Mts. and Smrčiny*. Knihovna ÚÚG 48, 120pp. [in Czech].
- Werner, O., Lippolt, H.J., Hess, J.C., 1997. Isotopische Randbedingungen zur Bestimmung der Alter tektonischer Prozesse im variscischen Erzgebirge. *Terra Nostra* 97/5, 199–204.
- Willner, A.P., Rötzler, K., Krohe, A., Maresch, W., Schumacher, R., 1994. Druck-Temperatur-Deformations-Entwicklung verschiedener Krustengesteine im Erzgebirge: Eine Modellregion für die Exhumierung von Krustengesteinen. *Terra Nostra* 3/94, 104–106.
- Willner, A.P., Rötzler, K., Maresch, W.V., 1997. Pressure–temperature and fluid evolution of quartzo–feldspathic metamorphic rocks with a relic high-pressure, granulite-facies history from the Central Erzgebirge (Saxony, Germany). *Journal of Petrology* 38, 307–336.